ELSEVIER

Heat Transfer and Heat Transfer Fouling in Kraft Black Liquor Evaporators

H. Müller-Steinhagen
Department of Chemical and Process Engineering, University of Surrey, Guildford, Surrey, United Kingdom

C. A. Branch
Chemical and Process Engineering Department, University of Newcastle, Newcastle upon Tyne, United Kingdom

■ A large number of experiments have been performed with New Zealand Forest Products Kraft black liquor to measure heat transfer coefficients and fouling rates during convective and subcooled flow boiling heat transfer as a function of surface temperature, bulk temperature, velocity, and solids concentration. Results from experiments with two chemical fouling inhibitors, with Teflon surface coating and in plate and frame heat exchangers, also are presented. The fouling deposits are analyzed with respect to appearance, composition, and process conditions for which they were obtained. With the assumption of chemical reaction–controlled fouling, a deposition model is developed and compared with the experimental data. © Elsevier Science Inc., 1997

Keywords: *evaporator fouling, Kraft black liquor, fouling mitigation, modelling*

INTRODUCTION

Pulp mills have always been confronted with organic and inorganic deposition and with corrosion. Fouling in multiple effect evaporators for Kraft pulp black liquor is caused by materials that are insoluble (such as fibers, sand, scale flakes, etc.), only moderately soluble ($CaCO_3$, silica, aluminum silicates) or highly soluble ($2Na_2SO_4$-Na_2CO_3) in the liquor [1–3]. Modern operation conditions have severely aggravated these problems. Increasing energy costs, stronger environmental control, and the trend toward higher yields has led to much higher levels of organic and inorganic solids circulating in the water system. Therefore, a knowledge of the basic mechanisms leading to deposition as well as an understanding of the governing process parameters have become essential for the design and economical operation of modern pulp mills.

At the New Zealand Forest Products' Kinleith pulp and paper mill, two different evaporator sets are used to concentrate the black liquor prior to combustion in the recovery furnace. They are the no. 4 and no. 5 multiple effect evaporator sets. The no. 4 set is a conventional rising film or long tube vertical unit with split feed. The no. 5 evaporator set is a very modern falling film design that incorporates flow switching in the final, high-concentration effects to minimize the extent of fouling. Figures 1 and 2 show the no. 4 and no. 5 evaporator set flow diagrams, respectively. To model the effect of fouling on the performance of the two evaporator sets, a modular computer code has been developed for the steady state performance [4, 5].

Number 4 Set Liquor Flow Pattern

Weak black liquor with a solids concentration of 15% is split between effects 5 and 6. The liquor fed to effect 5 is flashed and concentrated before being pumped to effect 6, where the process is repeated. This liquor is recombined with the other feed stream, which has passed through a separate flash and evaporation section in effect 6. The combined liquor stream is pumped through the effect 5 and 6 afterheaters before flowing from effects 4 to 1 in a standard countercurrent arrangement. The liquor leaving an effect passes through that effect's afterheater before being pumped to the next evaporator. Upon exiting effect 1, the liquor is flashed in a two-stage tank. This vapor is used as an extra source of heat in effects 3 and 4. Similarly, the clean condensate from effect 1 also is flashed, with the vapor providing extra heat for effects 2 and 4.

Number 5 Set Liquor Flow Pattern

Weak black liquor is pumped from the storage tanks and, if necessary, feed sweetened to a concentration of 18% solids with liquor from the intermediate black liquor tank. The liquor then enters dedicated flash sections in effects 5, 6, and 7. From effect 7, evaporation is carried out sequentially, in a backward feed manner. The final evaporation stage is in the first effect. This effect is fundamentally different from the preceding six effects. It consists of three subeffects that are linked in such a way as to accommodate variable liquor flow patterns between the

Address correspondence to Prof. H. Müller-Steinhagen, Department of Chemical and Process Engineering, University of Surrey, Guildford, Surrey, GU2 5XH, United Kingdom.

Experimental Thermal and Fluid Science 1997; 14:425–437

655 Avenue of the Americas, New York, NY 10010

0894-1777/97/$17.00
PII S0894-1777(96)00143-4

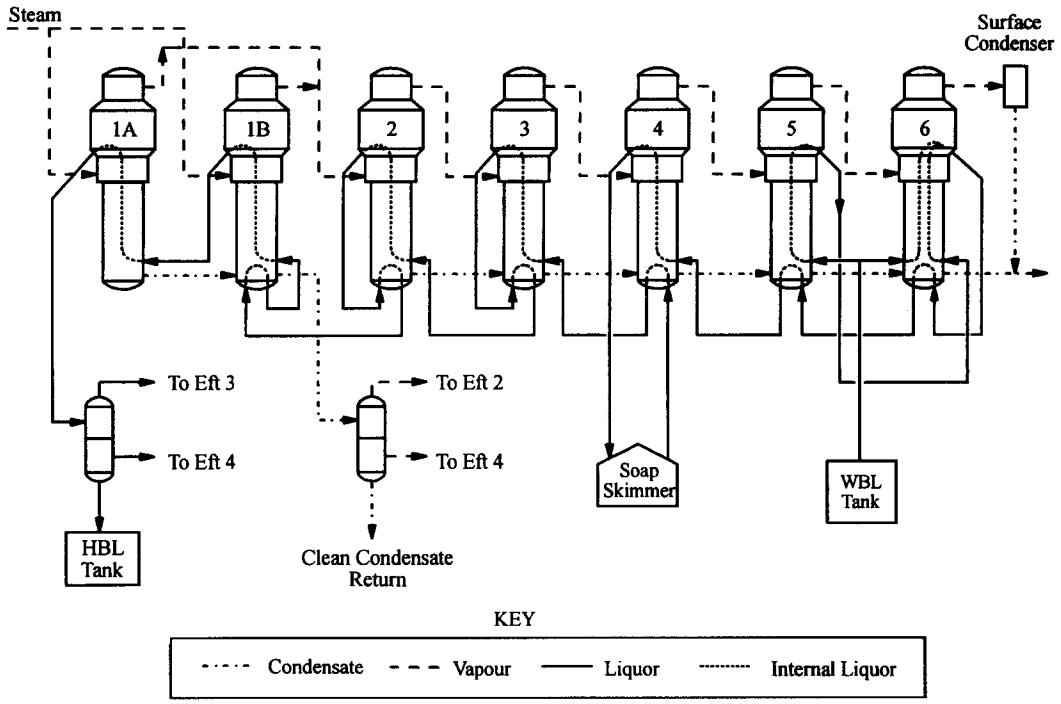

Figure 1. Number 4 evaporator set.

subeffects. The liquor flow pattern is switched at regular intervals to ensure that the heating elements are continually washed with incoming intermediate black liquor. This should prevent the buildup of scale on the heat transfer surfaces. Figure 3 shows, however, that the number of washing cycles required to maintain the design capacity of the high-concentration effect can escalate under certain operating conditions, making plant operation complicated and ineffective.

TEST APPARATUS AND EXPERIMENTAL PROCEDURE

Heat transfer measurements were performed with the experimental rig shown in Figure 4. The fluid was pumped from a temperature-controlled supply tank through a magnetic flowmeter to the test section, which consists of an annulus with a heated core. Details about the test section are given by Wenzel et al. [6]. The stainless steel-

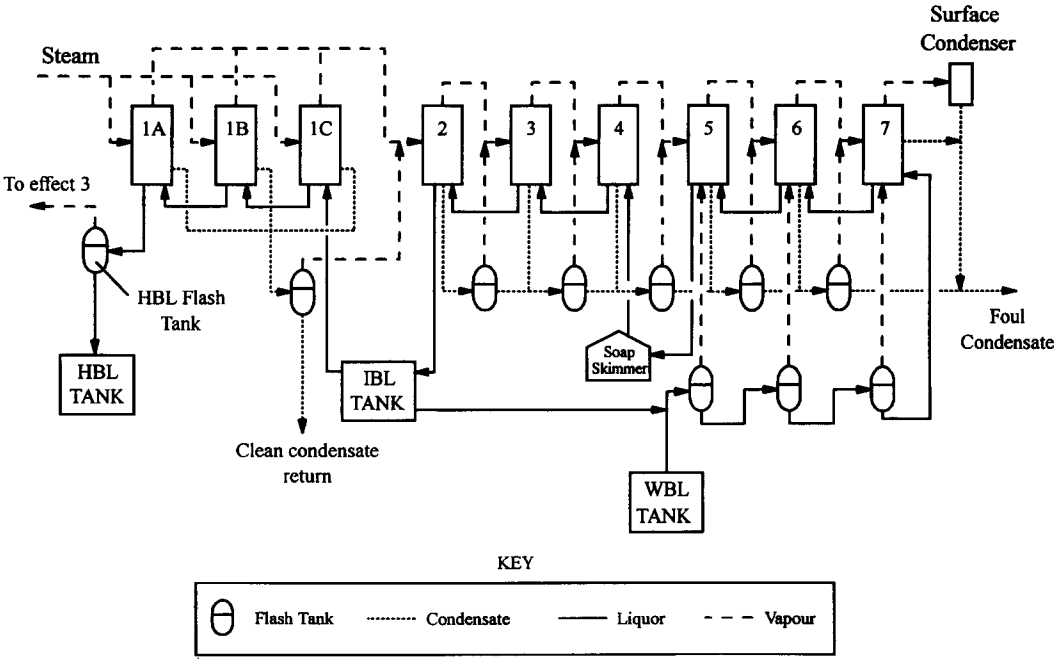

Figure 2. Number 5 evaporator set.

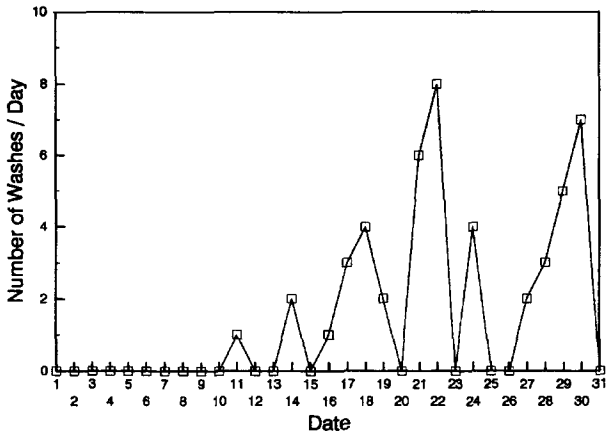

Figure 3. Number 1 effect weak black liquor washes per day.

sheathed electrical heater (HTRI design) is equipped with four thermocouples located close to the heating surface. The bulk temperature was measured with thermocouples located in mixing chambers before and after the test section. The flow rate was controlled with a gate valve before the test section and with the bypass line, which also ensured good mixing of the liquor in the tank. A 0 to 300 kPa pressure gauge was installed to measure the local pressure in the heated section, which could be altered by varying flow velocity and amount of bypass flow. The supply tank was maintained at a predetermined temperature with an internal cooling coil and temperature-controlled heating bands on the external surface. Nitrogen blanketing of the supply tank was used to avoid oxidation of the liquor during the experiments. The rig was fully insulated to minimize heat losses to the ambient air. Concentrated black liquor was obtained from New Zealand Forest Products' Kinleith mill in 60–100-L batches. Because of the variability of the liquor, results shown in diagrams in the next section were always obtained from the same sample.

The fouling resistance is calculated from the change in heat transfer coefficient with time:

$$R_f(t) - \frac{1}{\alpha(t)} - \frac{1}{\alpha_0}, \tag{1}$$

where α_0 is the initial "clean" heat transfer coefficient. The heat transfer coefficient was calculated from

$$\alpha = \frac{\dot{Q}}{A(T_w - T_b)}. \tag{2}$$

More details on the experimental procedure are given by Branch [7].

The composition of the fouling deposits was studied by two methods. The SEM/EDS (scanning electron microscope/energy dispersive X-ray analysis system) was used to look at the fine structure of the deposit, and, with the aid of the EDAX 9100 system, an elemental analysis of the deposit was obtained. X-ray diffraction was used to identify the different compounds present in a sample.

RESULTS

Heat Transfer Coefficients

Effect of Heat Flux Figures 5a and 5b show the effect of the heat flux on the heat transfer coefficient for liquor concentrations of 15% and 60%, respectively. The parameter in these diagrams is the flow velocity. One can clearly distinguish two different regimes, depending on the slope of the curves. In the convective heat transfer regime, the heat transfer coefficient is only slightly dependent on the heat flux but strongly dependent on the velocity. In contrast, the heat transfer coefficient increases with increasing heat flux in the nucleate boiling regime but is independent of the velocity. The slight variation of the heat transfer coefficient with heat flux for the convective heat transfer regime as seen in Figure 5b is a result of superposed natural convection currents and changes of the

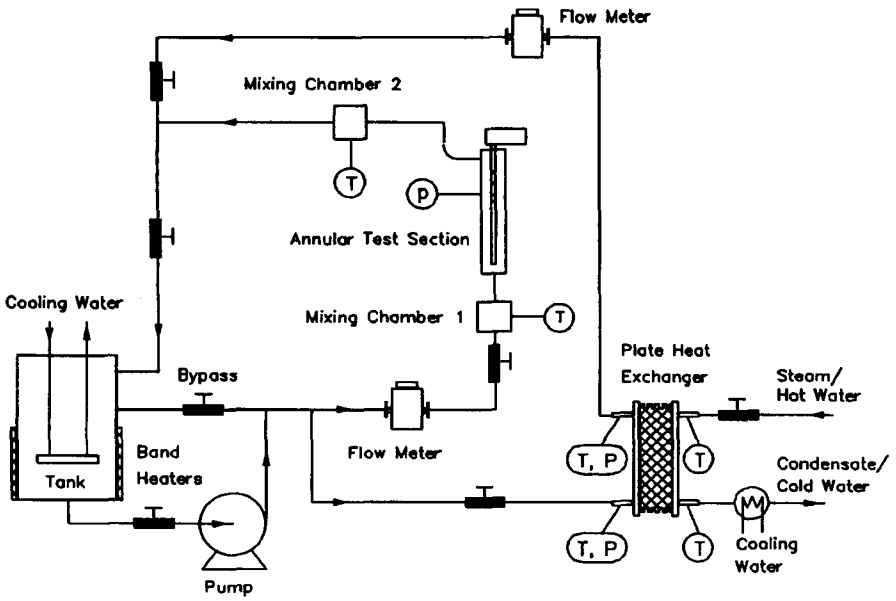

Figure 4. Schematic of experimental rig.

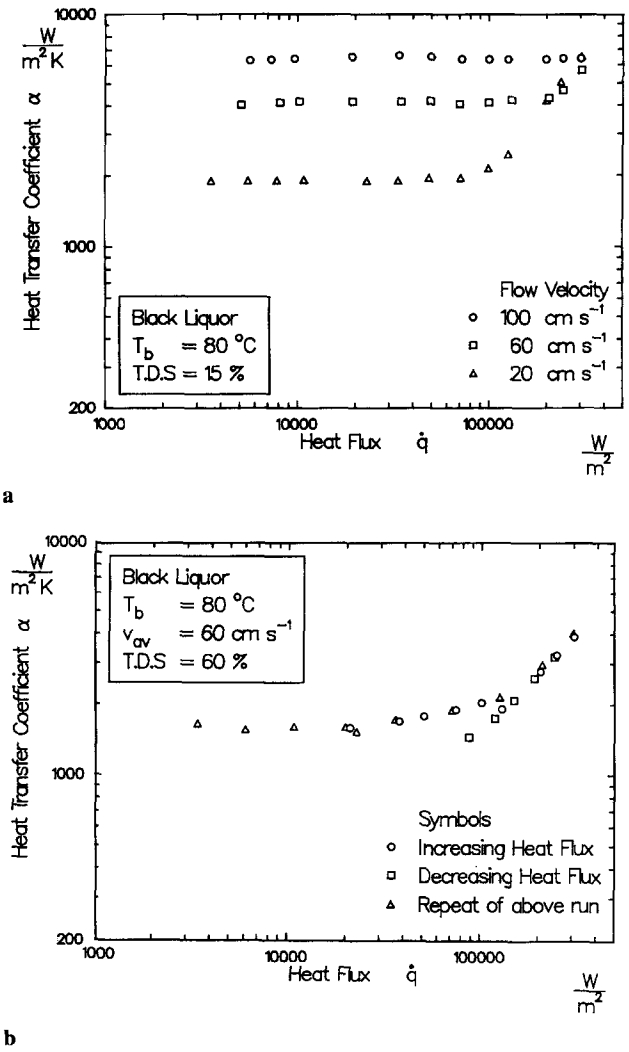

Figure 5. Heat transfer coefficient as a function of the heat flux for (a) 15% black liquor and (b) 60% black liquor.

physical properties of the solution, both as a result of the increased wall superheat.

Effect of Solids Concentration The solids concentration has a major effect on the physical properties of the solution. Physical properties of Kraft black liquor can be found in Ref. 8. For the present investigations, the Prandtl number varied between 2 and 500, the major contribution being the variation of the viscosity. All measured *convective* heat transfer coefficients are shown in Figure 6 as $Nu/Pr^{1/3}$ versus Reynolds number. The fact that all data can be approximated by a single line indicates the validity of a Prandtl exponent of 0.33. To eliminate the effect of wall superheat on the measured heat transfer coefficients, the heat flux for these experiments was adjusted such that the value of μ_b/μ_w was close to 2.

The measured *subcooled boiling* heat transfer coefficients decreased with increasing solids concentration for constant flow velocity and heat flux.

Effect of Flow Velocity Figure 6 shows three distinctive regimes with respect to the effect of Reynolds number on heat transfer—namely, laminar, transition, and turbulent flow regimes. For laminar flow, the following approximate relation is obtained:

$$Nu_{lam} = c_1 Re^{0.45}. \quad (3)$$

This is consistent with heat transfer with simultaneously developing hydraulic and thermal boundary layers [9]. For turbulent flow, the Nusselt-Reynolds relation can be approximated by

$$Nu_{turb} = c_2 Re^{0.8}, \quad (4)$$

which indicates fully developed turbulent flow [10–12]. A transition region exists for Reynolds numbers between 2000 and 4000.

Correlation of Data The measured heat transfer coefficients were compared with the predictions of a calculation procedure outlined in Ref. 13. Basically, this calculation procedure consists of a superposition of convective heat transfer—Shah and London [9] and Gnielinski [10] correlations—and boiling heat transfer—Gorenflo [14] correlation—according to a Chen model [15]. Excellent agreement between measured results and correlations was found for turbulent convective heat transfer and for the boiling regime. The 350 convective heat transfer data could be reproduced with an root-mean-square (RMS) error of 7%. Figure 7 shows a comparison between measured and predicted heat transfer coefficients for subcooled flow boiling, with an RMS value of 8%.

Fouling

The shape of a typical fouling curve is shown in Fig. 8. The initial fouling period shows a long delay time, which is known as the initiation period. In this period, nucleation sites for crystal growth are forming. Beyond the delay time, the fouling curve shows a linear increase with time. Note that there is a transition region between the initiation and linear periods.

Effect of Liquor Solids Concentration Most chemical pulping mills try to maintain their final liquor solids concentration above 65% to achieve high thermal efficiency and low emission of odor in the subsequent recovery boilers. However, it is not uncommon for a mill that is experiencing serious fouling problems to be producing liquor with lower concentration. The effects of concentration on fouling rates are strong. Figure 9 shows a comparison of the fouling for three concentrations. The difference between the fouling rates of the 65% liquor and the 60% liquor is approximately two orders of magnitude. No fouling was observed for the 55% liquor. The delay time also is strongly affected by the liquor solids concentration. It is possible that an excursion into rapid fouling may ultimately happen even for the 55% liquor, even though this has not been observed in experiments lasting as long as 1 week.

Effect of Surface Temperature and Flow Velocity Experiments have been performed on a 65% black liquor for various surface temperatures and flow velocities. Velocity effects are shown in Fig. 10 for constant surface and bulk

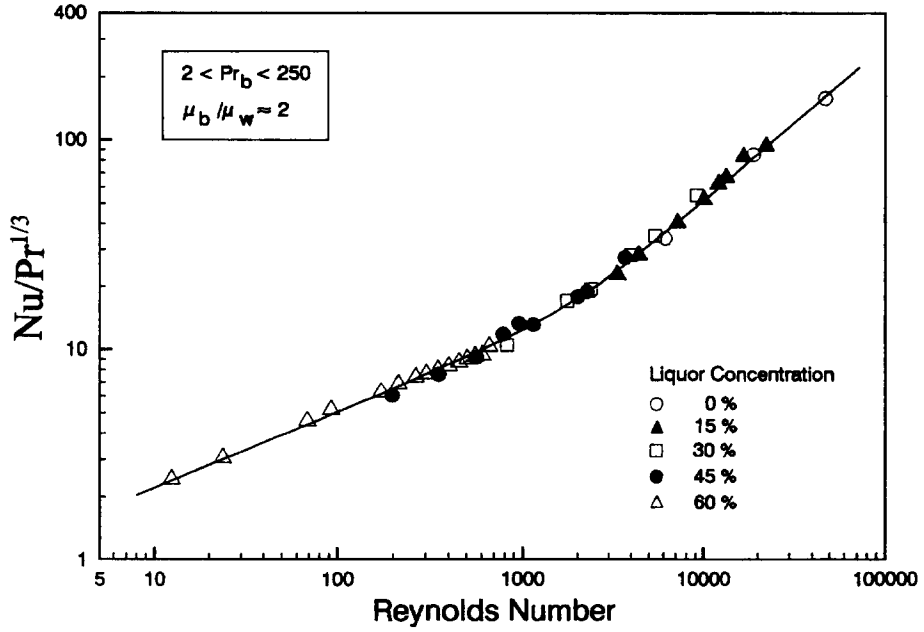

Figure 6. $Nu/Pr^{1/3}$ as a function of Reynolds number.

temperatures. For all velocities, the linear fouling rate remained essentially constant. This indicates that the deposition rate is independent of the flow velocity. This result is characteristic for chemical reaction-controlled fouling. The delay time is seen to be a function of the velocity, showing a maximum for a velocity of about 50 cm/s. It is unclear how the velocity affects the nucleation kinetics and, without information on the process of nucleation site formation, the experiments do not permit conclusions to be drawn on this. However, delay times in industrial applications are normally observed during the initial commissioning of new heat transfer equipment. After this period, the surface characteristics generally change, and the delay time is either significantly reduced or no longer observed.

Results shown in Fig. 11 illustrate that induction (initiation) period and fouling rate depend strongly on the surface temperature. The fouling rate increases and the delay time decreases with increasing surface temperature. It should be noted that convective heat transfer occurred for the experiments at low surface temperatures; at high surface temperatures, nucleate boiling prevailed. The effect of surface temperature on the delay time may be expressed by the following correlation:

$$\frac{1}{t_d} = k_d \exp\left(\frac{-E_{act}}{R \cdot T_s}\right), \tag{5}$$

$$k_d = 2.444 \times 10^{20}\ \text{min}^{-1}, \tag{6}$$

$$E_{act} = 1.647 \times 10^5\ \text{J/mol}. \tag{7}$$

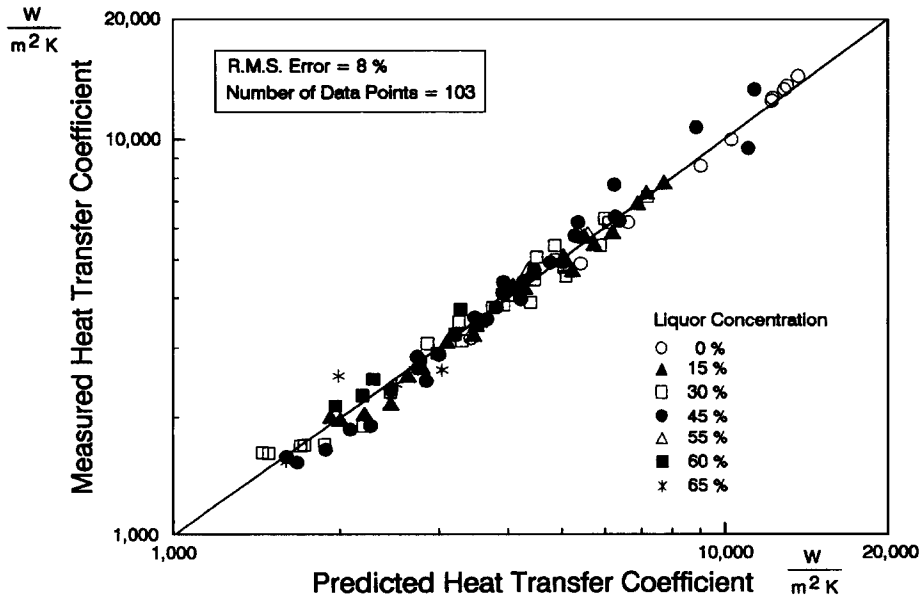

Figure 7. Measured and predicted subcooled boiling heat transfer coefficients.

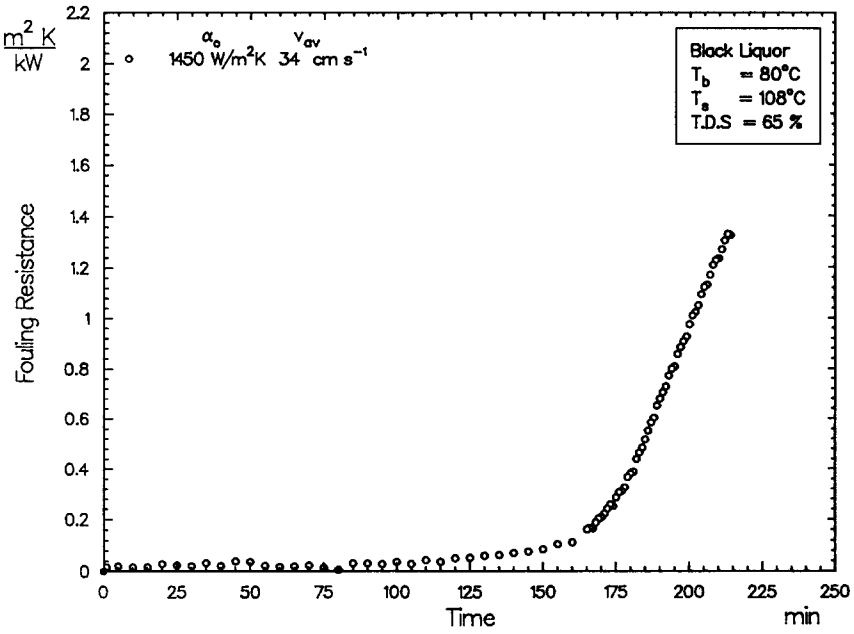

Figure 8. Typical fouling curve.

Figure 11 shows no fouling for the run with a surface temperature of 87°C. This experiment was stopped after 24 h. Equations (5)–(7) predict that the run would have had to be continued for 52 h before the first signs of fouling may have appeared.

Effect of Subcooling The effect of bulk temperature is shown in Figure 12. For a constant surface temperature and velocity, the rate of fouling increases with decreasing bulk temperature, probably as a result of the decreasing solubility of the scale-forming components. For the three runs where fouling was observed, the delay time remains almost constant with bulk temperature, suggesting that delay time depends on surface rather than bulk conditions. It is open to speculation whether deposits may start to form in the experiment at 100°C bulk temperature after a greatly prolonged delay period.

Figure 13 shows a series of experiments obtained for a bulk temperature of 108°C and surface temperatures more than 25 °C higher than the results presented in Figure 12. Under these conditions, bubble formation on the heat transfer surface occurs. The fouling curves start with a constant rate of deposition with no delay time. These fouling curves suggest a different mechanism from that discussed above. For subcooled and saturated boiling, the number of active bubble nucleation sites is increased with increasing wall superheat. Deposition can occur from the concentrated regions under a growing bubble, owing to

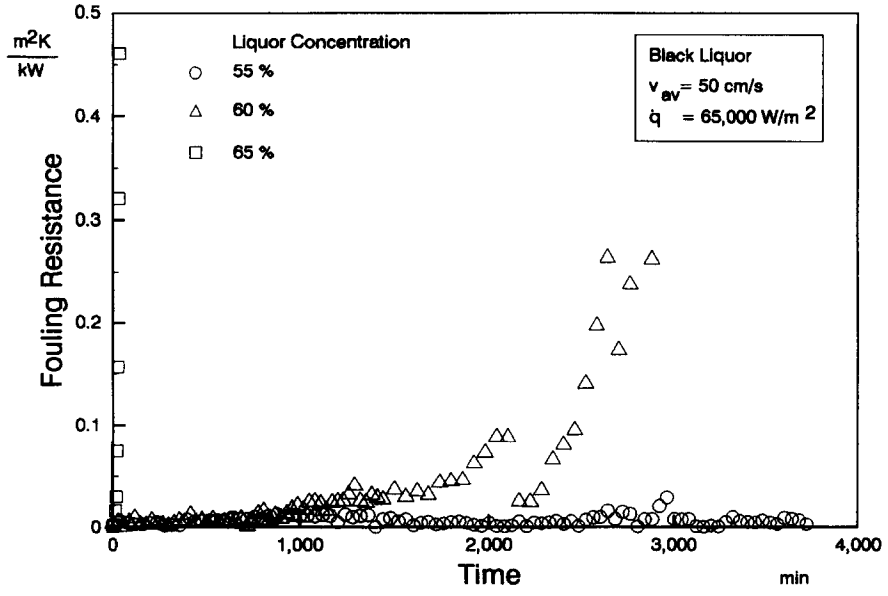

Figure 9. Effect of liquor concentration on fouling rates.

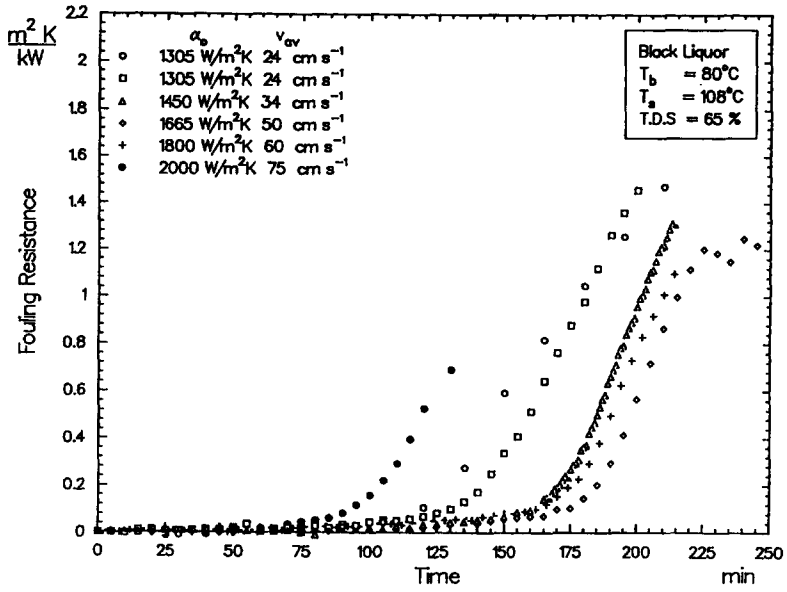

Figure 10. Effect of flow velocity on fouling rates.

the mechanism of microlayer evaporation [16]. Evidence of the microlayer deposition mechanism was found by prematurely stopping a high heat flux fouling experiment. A large number of tiny rings were found on the heat transfer surface, the size of these rings being of the same order as the bubble departure diameter. Obviously, the deposition rate from microlayer evaporation must increase with the number of active bubble nucleation sites on the heat transfer surface. For the low wall or bulk temperature experiments or both, few or no nucleation sites would have been active, and hence the microlayer deposition mechanism would not have been significant. This is the reason for the delay times required for crystal nucleation. In contrast, the large number of active nucleation sites for the high wall and bulk temperature experiments leads to remarkable initial deposition rates.

Appearance of Deposit Deposits obtained from the fouling experiments have a smooth appearance and are strongly bonded to the heating surface. In all cases, the deposits had a thin layer of what appeared to be black liquor immediately adjacent to the heating surface. For all experiments, the deposit was completely soluble in water, thus indicating a carbonate–sulfate type scale. It was noticed that high heat flux fouling experiments generally gave highly porous scales.

Scanning electron micrographs obtained from two different experiments are shown in Figs. 14 and 15. The micrographs show the structure of the deposit on the heat transfer surface. Figure 14 shows a uniform crystalline structure with the growth of the deposit from nucleation sites. Figure 15 shows a deposit with a much less defined crystal structure. Such variations in the morphology are a

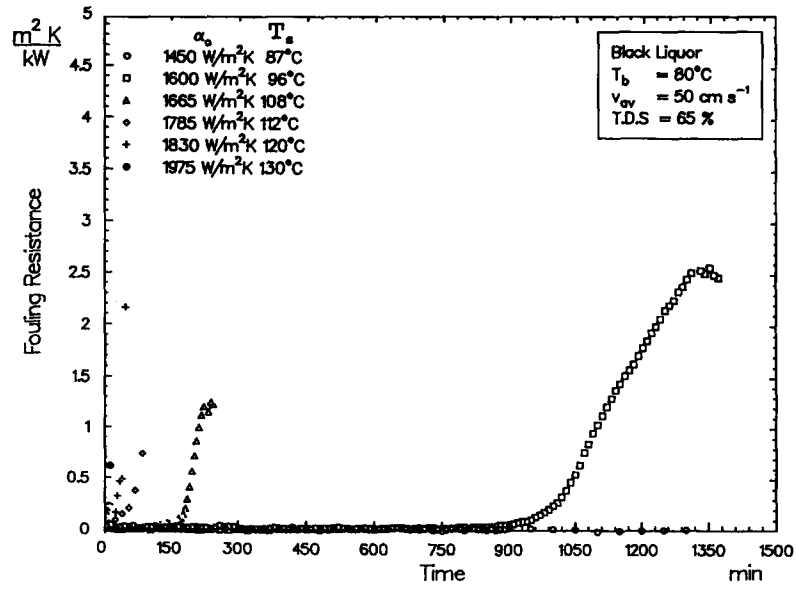

Figure 11. Effect of surface temperature on fouling rates.

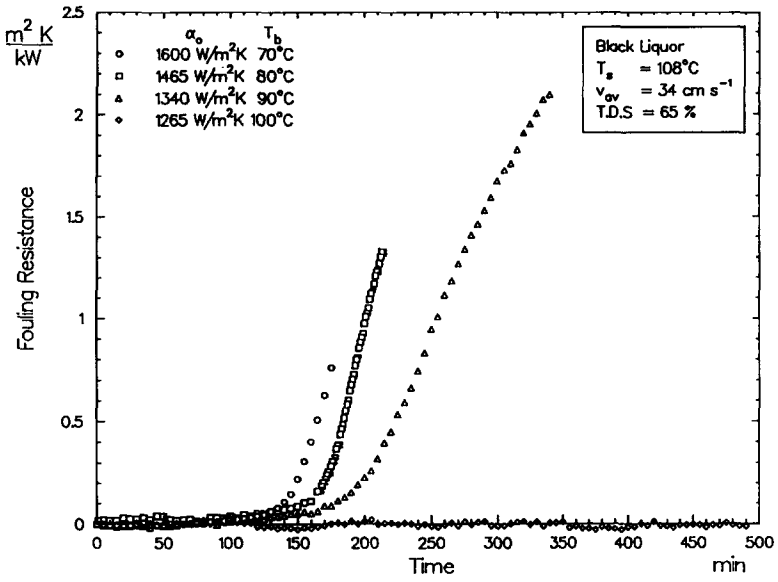

Figure 12. Effect of bulk temperature on fouling rates.

result of the different types of deposition for each sample. The deposit in Fig. 14 was formed with a long delay time, which perhaps explains the distinctive crystal growth. In contrast, the deposit in Fig. 15 was formed by very rapid deposition with no noticeable delay time. It is thought that the rapid deposition rate may not allow the crystal structure to develop to the extent of the Fig. 14 deposit.

Analyses EDAX analysis of black liquor provides its major elemental composition. A sample of 65% black liquor was oven dried for 24 h at 105°C. The major elements identified are sodium, potassium, sulfur, and silicon. A large peak near the silicon and sulfur positions could indicate aluminum. Calcium also may be present, although the sample did not show it clearly. Elemental analyses of the deposits from Figs. 14 and 15 show that the deposits contain mainly sodium and sulfur.

Diffraction experiments were performed by using a Philips X-ray diffractometer system. This system consists of a PW 1729 X-ray generator, a PW 1050 vertical goniometer, a PW 1771 diffractometer, a 1133 sample spinner (120 rpm), a PW 1752 curved graphite monocrometer, a xenon sealed proportional detector, a PW 1710 diffractometer control unit, and a PM 8203A online recorder. The wavelength of the X-ray source was 1.791×10^{-10} m. From all the deposits analyzed, the following compounds were identified: Na_2CO_3, $Na_2S \cdot H_2O$, Na_2S_2, $Na_6CO_3(SO_4)_2$ (Burkeite), $K_2Ca(CO_3)_2$, and $CaCO_3$. This analysis shows that the deposits consist mostly of Burkeite

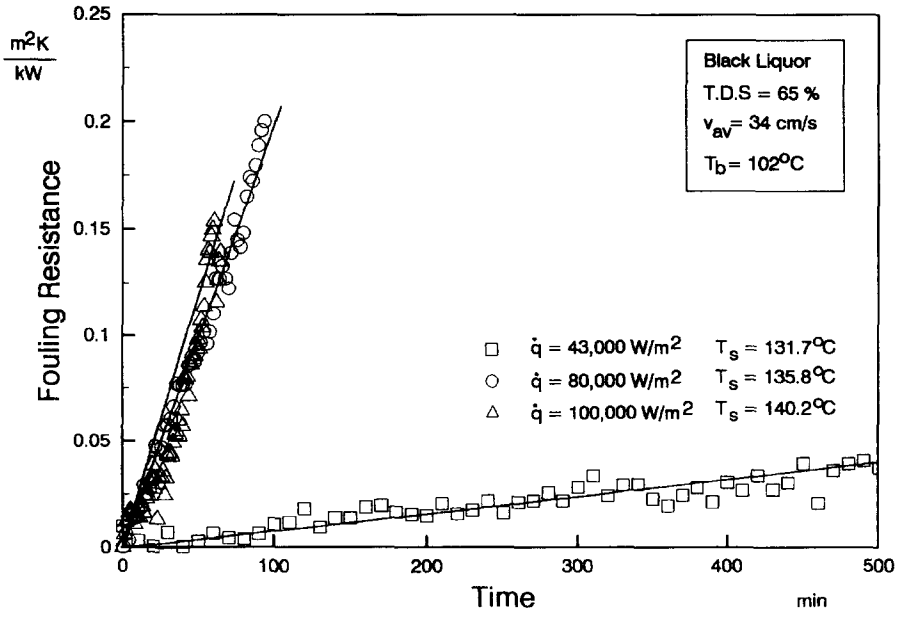

Figure 13. Fouling resistance versus time for low subcooling with varying surface temperature.

combined with a pseudosteady-state simulation model [4, 5] for the performance of the multiple effect evaporators at the New Zealand Forest Products Kinleith mill.

Equations (11) and (17) can be used to evaluate the effects of process parameters on fouling in an industrial evaporator. In most industries, it is important to maintain the product solids concentration. Under fouling conditions, this is usually done by increasing the steam pressure. For this case, a constant heat flux is maintained and Eq. (11) applies. From Eq. (11), the fouling is minimized by maintaining a low surface temperature and a small temperature difference. The velocity will have little effect. The initiation of a cleaning cycle is dependent on the available steam pressure and the tolerable drop in solids concentration.

Some evaporators are already operating at the maximum steam temperature. For these situations, the fouling continually reduces the surface temperature and Eq. (17) applies. Although the reaction rate is independent of velocity, an increase in velocity for convective heat transfer will increase the heat transfer coefficient, which will reduce the overall rate of fouling. However, for nucleate boiling conditions, the heat transfer coefficient is independent of velocity and as such there is no velocity effect. Again, low surface temperatures and small temperature differences minimize the fouling rate. For evaporators operating with a fixed steam temperature, the fouling will strongly affect the product solids concentration. After a minimum acceptable concentration has been reached, a cleaning cycle must be initiated.

Epstein [18] analyzed scaling governed by Eq. (17). The analysis optimizes the maximum daily production operating cycle, assuming a fixed cleaning time, t_{clean}. The result of his analyses is given in Eq. (18) for the optimum evaporator time as a function of the down time for cleaning.

$$t_{evp}^{opt} = t_{clean} + \sqrt{\frac{2t_{clean}}{\alpha_0\left(\frac{\partial R_f}{\partial t}\right)_{t=0}}} \qquad (18)$$

With the use of Eq. (18), optimal operating times can be obtained. For assumed operating conditions of t_{clean} = 120 min, α = 2000 W/(m^2 K), T_s = 135°C and T_b = 120°C, Eqs. (16) and (18) predict an optimum operating time of 220 min, which is close to plant practice. Most modern black liquor evaporators have a parallel setup in the effects where fouling occurs. For these effects, when one evaporator is down for cleaning, the other is still online. Hence a continuous switching between evaporators is occurring. For the optimal case discussed above, the parallel effects would have to be switched twice per 8-h operator shift.

REDUCTION OF FOULING

Chemical Treatment to Reduce Scale Formation

There are a number of chemical treatments for fouling in black liquor systems, most being specific to calcium carbonate scaling. Two proprietary chemicals were tested to find their performance in preventing fouling from New Zealand Forest Products' Kinleith black liquor. The results cannot be extrapolated to other liquors.

The two chemicals investigated were coded S62-2 and S89-2. Recommended dosage for once-through processes is 25 ppm. Based on the recommended dosage, a 65% solids liquor that caused considerable fouling was tested with each of the chemical additives.

Figure 16 shows a comparison of fouling from untreated and S62-2 treated liquor. It was found that the recommended dosage only marginally reduced the fouling; the severe characteristic fouling rate was still observed in the final stages. Large improvements were noted for the 100-ppm and 200-ppm runs. Severe fouling was delayed until nearly seven times the untreated fouling time. In the 200-ppm treatment, no fouling escalation was observed for the 52-h duration of the run. From these results, it can be concluded that the S62-2 chemical treatment may be used to reduce the fouling potential of Kinleith Kraft black liquor, it if is still economical at five to ten times the initially recommended dosage.

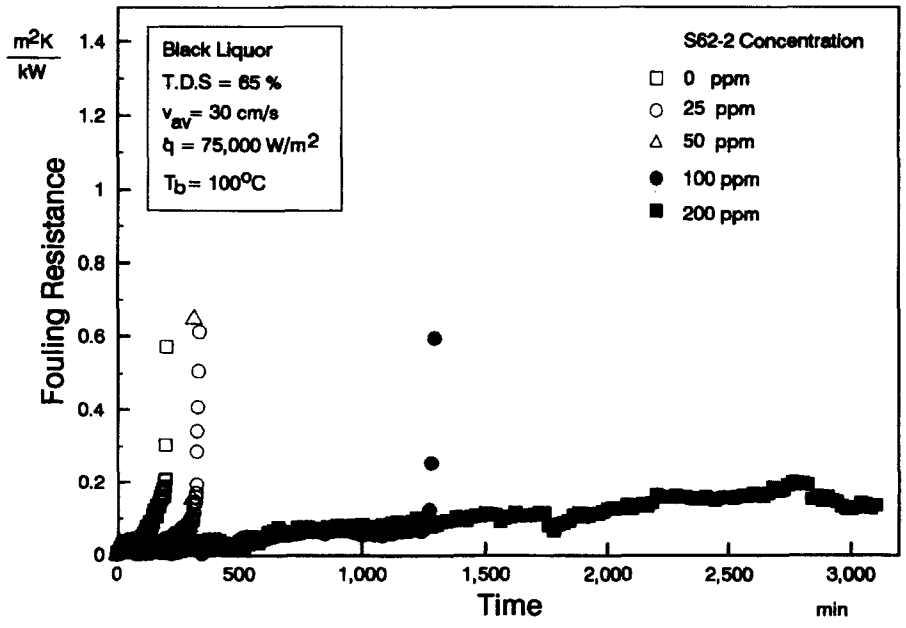

Figure 16. Fouling resistance versus time for varying S62-2 concentrations.

Figure 17 shows the effect of chemical treatment for the same 65% solids black liquor with various S89-2 concentrations. The chemical treatment with S89-2 began with the recommended dosage of 25 ppm. Severe fouling was then observed earlier than in the untreated case. The same trend was observed for further increases in concentration. The results clearly show that S89-2 greatly aggravates fouling.

Surface Coating with Teflon

Attempts were made to reduce the stickiness of the deposit by coating the heat transfer surface with PTFE. Figure 18 shows a strong sawtooth character. The time until severe fouling occurred was significantly prolonged. When the fouling has grown to a resistance of about 0.15 m^2 K/kW, the deposit sloughs. The average period of removal is estimated at 15 min. Note that, beyond 300 min, the sloughing diminishes. This suggests that the continual removal of deposit may wear down the Teflon coating. A practical Teflon coating must have better durability than the coatings used in this investigation.

Plate and Frame Heat Exchanger

Plate heat exchangers provide a large wall shear stress and high heat transfer coefficients. This may reduce deposition by increasing deposit removal rates and reducing surface temperature. A number of fouling experiments were performed with an α-Laval PO1 plate heat exchanger for a 68% solids black liquor, which rapidly fouled the annular test section for comparable heat fluxes [19]. Each experiment lasted 24 h. For the investigated velocities (0.65 m/s and 1.0 m/s) and surface temperatures (114.5°C and 128.5°C), no fouling was observed.

CONCLUSIONS

Measurements have been presented for forced convective and subcooled flow boiling heat transfer to Kraft black liquor with dissolved solids concentrations between 15% and 65%. All experimental data can be predicted with good accuracy by using well-known correlations.

Water-soluble deposits from Kraft black liquor are very sensitive to the liquor solids concentration. For high concentration liquors ($\geq$ 65%), the rate of deposition is rapid. Deposition rates increase with increasing surface temperature and decreasing bulk temperature. The fouling process is insensitive to variations in velocity, at least over the observed range of flow rates. The heat transfer mechanism (convection versus nucleate boiling) considerably affects the mechanism of fouling. The investigated deposits are porous and contain fibers. The rate of deposition affects the crystal morphology, with high rates of deposition resulting in less well defined crystal structure.

The modeling of the deposition process with a chemical reaction fouling model allows discussion of the effects of a number of process parameters on the fouling rates. Under both constant heat flux and constant sensible heat transfer modes, fouling is reduced by minimizing the surface temperature and the surface-to-bulk temperature difference. The fouling model can be used to estimate optimal cleaning cycles of black liquor evaporators.

Chemical treatment of high concentration liquors can reduce their fouling potential. However, it is advisible to perform preliminary laboratory experiments under comparable conditions, to prevent adverse effects. Surface coating with Teflon reduces the overall fouling rate. Plate and frame heat exchangers are less prone to fouling from Kraft black liquor than are tubular heaters.

The authors are indebted to PAPRO NZ and to New Zealand Forest Products Ltd. for continuous support of the investigations.

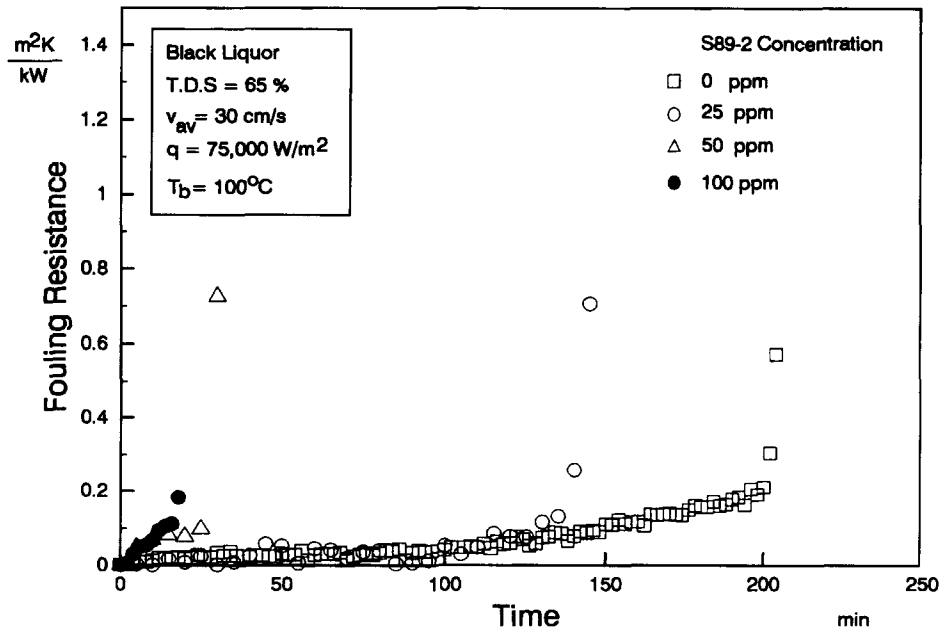

Figure 17. Fouling resistance versus time for varying S89-2 concentrations.

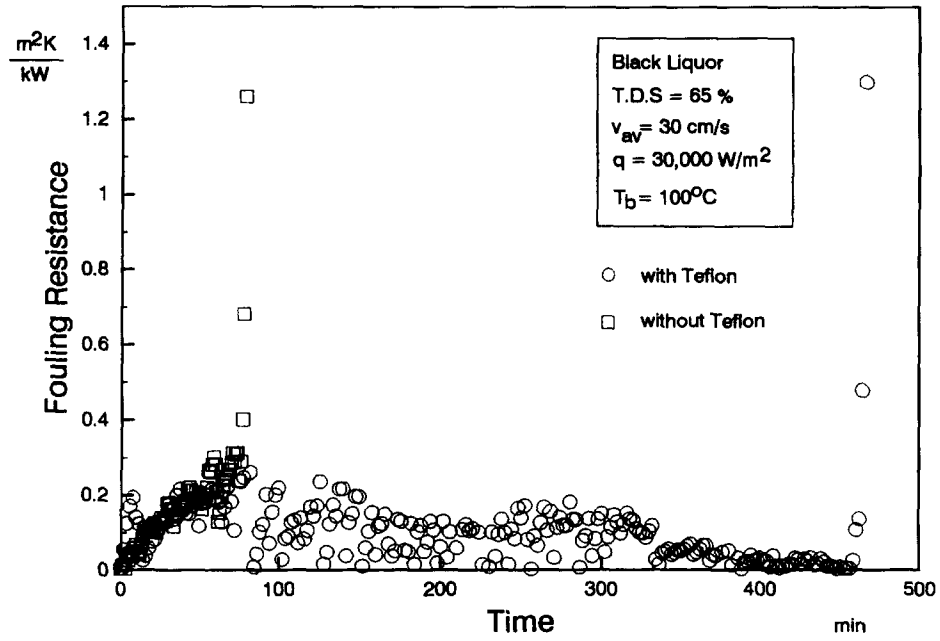

Figure 18. Effect of Teflon coating on fouling.

NOMENCLATURE

a	heat transfer surface area, m^2
$c_{1,2}$	constants
c_b	concentration in bulk, kg/m^3
c_p	specific heat capacity, J/(kg K)
c_s	concentration at surface, kg/m^3
d	diameter, m
e	exponent in Eqs. (11) and (14)
j	j-factor
E_{act}	activation energy, J/mol
K	Arrhenius constant, $(kg/m^2\ min)/(kg/m^3)^e$
k_c	fouling rate constant, $kg(m^3\ K)$
k_d	reaction rate constant, min^{-1}
k_r	reaction rate constant, $(kg/m^2\ min)/(kg/m^3)^e$
m	deposit mass per area, kg/m^2
Nu	Nusselt number ($= \alpha d/\lambda$)
Nu_{lam}	Nusselt number for laminar flow
Nu_{turb}	Nusselt number for turbulent flow
n	exponent in Eq. (8)
Pr	Prandtl number ($= \mu c_p/\lambda$)
$\dot{q}$	heat flux, W/m^2
$\dot{Q}$	heat flow rate, W
R	universal gas constant, 8.314 J/(mol K)
Re	Reynolds number ($= vd/\nu$)
R_f	fouling resistance, m^2 K/kW
T_b	bulk temperature, °C
T_s	deposit—fluid interface temperature, °C
T_w	heat transfer wall temperature, °C
t	time, min
t_{clean}	cleaning time, min
t_d	delay time, min
v_{av}	average flow velocity, m/s

Greek Symbols

α	heat transfer coefficient, $W/(m^2\ K)$
α_0	clean heat transfer coefficient, $W/(m^2\ K)$
λ_d	deposit thermal conductivity, W/(m K)
ρ_d	deposit density, kg/m^3
μ	dynamic viscosity, Pa s
ν	kinematic viscosity, m^2/s

Other

( ) function of

REFERENCES

1. Frederick, W. J., and Grace, T. M., Preventing Calcium Carbonate Scaling in Black Liquor Evaporators. *South. Pulp Paper Manuf.*, August, 22–24, September, 21–29, 1979.
2. Frederick, W. J., and Grace, T. M., Scaling in Alkaline Spend Pulping Liquor Evaporators. In *Fouling of Heat Transfer Equipment*, E. F. C. Somerscales and J. G. Knudsen, Eds., pp. 587–601, Hemisphere, Washington, DC, 1981.
3. Grace, T. M., Solubility Limits in Black Liquor Evaporators. *Pulp Paper* **41**(13), 42–43, 1967.
4. Bremford, D., and Müller-Steinhagen, H. M., Multiple Evaporator Performance for Black Liquor I: Simulation of Steady State Operation for Different Evaporator Arrangements. *APPITA J.* **47**(4), 320–326, 1994.
5. Bremford, D., and Müller-Steinhagen, H. M., Multiple Effect Evaporator Performance for Black Liquor II: Simulation of Dynamic Operation and Methods of Increasing the Final Liquor Concentration. *APPITA* **49**(5), 337–346, 1996.
6. Wenzel, U., Hartmuth, B., and Müller-Steinhagen, H. M., Heat Transfer to Ternary Mixtures of Acetone, Isopropanol, and Water under Subcooled Flow Boiling Conditions I: Experimental Results. *Int. J. Heat Mass Transfer* **37**(2), 175–183, 1994.
7. Branch, C. A., Fouling During the Evaporation of Kraft Black Liquor. PhD Thesis, Univ. Auckland, Auckland, New Zealand, 1992.
8. Branch, C. A., and Müller-Steinhagen, H. M., Physical Properties of Kraft Black Liquor. *APPITA J.* **44**(5), 339–341, 1991.
9. Shah, R. K., and London, A. L., *Laminar Flow: Forced Convection in Ducts*. pp. 284–319, Academic Press, New York, 1978.
10. Gnielinski, V., *Wärmeübertragung in Rohren, VDI-Wärmeatlas*. 5th ed., VDI-Verlag, Düsseldorf, 1986.

11. Dittus, F. N., and Boelter, L. M. K., *Heat Transfer in Automobile Radiators*. Vol. 2, p. 443, Univ. California Press, 1930.
12. Petukhov, B. S., Heat Transfer and Friction in Turbulent Pipe Flow with Variable Physical Properties. In *Advances in Heat Transfer*, J. P. Hartnett and T. F. Irvine, Eds., pp. 504–564, Academic Press, New York, 1970.
13. Müller-Steinhagen, H., and Jamialahmadi, M., Subcooled Flow Boiling Heat Transfer to Solutions and Mixtures. Engineering Foundation Conf. on Flow Boiling, Banff, Canada, 1995.
14. D. Gorenflo, *Behältersieden. VDI-Wärmeatlas*, Sect. Ha, 4th ed. VDI-Verlag, Düsseldorf, 1984.
15. J. C. Chen, Correlation for Boiling Heat Transfer to Saturated Fluids in Convective Flow. *Ind. Eng. Chem. Process Design Dev.* **5**, 322–329, 1966.
16. Jamialahmadi, M., Blöchl, R., and Müller-Steinhagen, H., Bubble Dynamics and Scale Formation During Boiling of Aqueous $CaSO_4$ Solutions. *Chem. Eng. Process* **24**, 15–26, 1989.
17. McCabe, W. L., and Robinson, C. S., Evaporator Scale Formation in Tubular Heat Exchanger. *Ind. Eng. Chem.* **16**(5), 478–479, 1924.
18. Epstein, N., Optimum Evaporator Cycles with Scale Formation. *Can. J. Chem. Eng.* **57**, 659–661, 1979.
19. Branch, C. A., Müller-Steinhagen, H., and Seyfried, F., Heat Transfer to Kraft Black Liquor in Plate Heat Exchangers. *APPITA J.* **44**(4), 270–272, 1991.

Received April 17, 1996; revised August 15, 1996